

Momentum Distribution of the Homogeneous Electron Gas

Markus Holzmann,^{1,2} Bernard Bernu,² Carlo Pierleoni,³ Jeremy McMinis,⁴ David M. Ceperley,⁴
Valerio Olevano,⁵ and Luigi Delle Site⁶

¹*Université Grenoble 1/CNRS, LPMMC UMR 5493, Maison des Magistères, 38042 Grenoble, France*

²*LPTMC, UMR 7600 of CNRS, UPMC, Jussieu, Paris, France*

³*Physics Department, University of L'Aquila, Via Vetoio, 67100 L'Aquila, Italy*

⁴*Department of Physics and NCSA, University of Illinois at Urbana-Champaign, Urbana, Illinois 61801, USA*

⁵*Institut Néel, Grenoble, France*

⁶*Max-Planck-Institute for Polymer Research, Ackermannweg 10, D 55021 Mainz, Germany*

(Received 18 May 2011; revised manuscript received 6 July 2011; published 8 September 2011)

We calculate the off-diagonal density matrix of the homogeneous electron gas at zero temperature using unbiased reptation Monte Carlo calculations for various densities and extrapolate the momentum distribution and the kinetic and potential energies to the thermodynamic limit. Our results on the renormalization factor allow us to validate approximate G_0W_0 calculations concerning quasiparticle properties over a broad density region ($1 \leq r_s \leq 10$) and show that, near the Fermi surface, vertex corrections and self-consistency aspects almost cancel each other out.

DOI: 10.1103/PhysRevLett.107.110402

PACS numbers: 05.30.Fk, 02.70.Ss, 71.10.Ay, 71.10.Ca

The uniform electron gas (jellium) is one of the most fundamental models for understanding electronic properties in simple metals and semiconductors. Knowledge of its ground state properties and, in particular, of modifications due to electron correlation is at the heart of all approximate approaches to the many-electron problem in realistic models. Quantum Monte Carlo methods (QMC) [1] have provided the most precise estimates of the correlation energy, electron pair density, and structure factor of jellium, basic quantities for constructing and parametrizing the exchange-correlation energy used in density functional theory [2].

Correlations modify the momentum distribution, n_k , of electrons, and introduce deviations from the ideal Fermi-Dirac step function. The magnitude of the discontinuity at the Fermi surface (k_F), the renormalization factor Z , quantifies the strength of a quasiparticle excitation [3] and plays a fundamental role in Fermi liquid and many-body perturbation theory (GW) for spectral quantities. Whereas the momentum distribution (as well as other spectral information) is inaccessible in current Kohn-Sham density functional theory formulations, the reduced single-particle density matrix—the Fourier transform of n_k in homogeneous systems—is the basic object in the so-called density-matrix functional theory [4]; this theory relies on knowledge of n_k of jellium. Inelastic x-ray scattering measurement of the Compton profile of solid sodium [5] has determined n_k , but experiments for elements with different electronic densities are less conclusive.

In this Letter, we calculate n_k for the electron gas (jellium) by QMC calculations in the density region $1 \leq r_s \leq 10$. Here, $r_s = (4\pi n a_B^3/3)^{-1/3}$ is the Wigner-Seitz density parameter, n is the density, and $a_B = \hbar^2/me^2$ is the Bohr radius. In contrast to previous calculations [6], our

calculations are based on more precise backflow (BF) wave functions [7], and a careful extrapolation to the thermodynamic limit [8,9]. Similar to the worm algorithm in finite temperature path-integral and lattice Monte Carlo [10,11] calculations, we have extended reptation Monte Carlo (RMC) calculations [12] to include the off-diagonal density matrix in order to obtain an unbiased estimator of the momentum distribution [13,14]. From our extrapolation scheme, we derive the exact behavior of n_k close to the Fermi surface. By comparing the renormalization factor, Z , with different approximate GW theories, we can judge the importance of self-consistency and vertex corrections within these approaches. The excellent agreement of our QMC results with G_0W_0 over a broad density region indicates strong cancellations of vertex and self-consistency corrections close to the Fermi surface.

Within variational Monte Carlo (VMC) calculations, the ground state wave function is approximated by a trial wave function, $\Psi_T(\mathbf{R})$, whereas within projector Monte Carlo methods, e.g., diffusion Monte Carlo (DMC) or RMC calculations, the trial state is improved using $\Psi_\beta \propto \exp[-\beta H]\Psi_T$; this converges exponentially fast to the true ground state for increasing projection time β . To circumvent the so-called fermion sign problem, calculations are done within the fixed-node approximation, introducing small systematic deviations from the exact fermion ground state [15]. Whenever the (approximate) nodes of the system are described by a determinant of single-particle orbitals $\phi_n(\mathbf{r})$, the (fixed-node) ground state wave function, $\Psi_N(\mathbf{R})$, of N particles at positions $\mathbf{R} \equiv \{\mathbf{r}_i\}$ can be written as

$$\Psi_N(\mathbf{R}) = D_N \exp[-U_N], \quad D_N = \det_{nl} \phi_n(\mathbf{r}_l + \nabla_l W_N), \quad (1)$$

where W_N and U_N are generalized backflow and Jastrow potentials [16], respectively.

From an approximate ground state wave function, $\Psi_N(\mathbf{R})$, we obtain the reduced single-particle density matrix [17]

$$f_N(\mathbf{r}) = \langle F(\mathbf{R}; \mathbf{r}) \rangle_N, \quad F = \frac{1}{N} \sum_i \frac{\Psi_N(\mathbf{R}; \mathbf{r}_i + \mathbf{r})}{\Psi_N(\mathbf{R})}, \quad (2)$$

where $\mathbf{R}; \mathbf{r}_i + \mathbf{r}$ indicates that the position of particle i is displaced by \mathbf{r} , and $\langle \dots \rangle_N \equiv \int d\mathbf{R} \dots |\Psi_N|^2 / Q$ with $Q \equiv \int d\mathbf{R} |\Psi_N|^2$ playing the role of a partition function. The Fourier transform of $f_N(\mathbf{r})$ directly yields the momentum distribution, $n_{\mathbf{k}}^N$, of the electrons per spin

$$n_{\mathbf{k}}^N = \frac{1}{2V} \int d\mathbf{r} e^{-i\mathbf{k} \cdot \mathbf{r}} f_N(\mathbf{r}), \quad (3)$$

where V is the volume.

The large variance of the estimator of the off-diagonal density matrix, Eq. (2), makes precise calculations very time-consuming. To reduce the variance for homogeneous systems with plane wave orbitals, $\phi_n(\mathbf{r}) \propto e^{i\mathbf{k}_n \cdot \mathbf{r}}$, we separate the ideal gas density matrix, $f_{\text{id}}(\mathbf{r}) = \sum_n \phi_n^*(\mathbf{r}) \phi_n(0) / \sum_n |\phi_n(0)|^2$, based on the estimator

$$F_{\text{id}}(\mathbf{R}; \mathbf{r}) = \frac{1}{N} \sum_i \frac{D_N(\mathbf{R}; \mathbf{r}_i + \mathbf{r}; W_N(\mathbf{R}))}{D_N(\mathbf{R}; W_N(\mathbf{R}))}, \quad (4)$$

where the determinants on the right-hand side of Eq. (4) are evaluated using the backflow coordinates, $W_N(\mathbf{R})$, of the diagonal configuration \mathbf{R} with undisplaced particle coordinates. Expanding it around $\mathbf{r} = 0$, we can explicitly verify that $f_{\text{id}}(\mathbf{r}) = \langle F_{\text{id}}(\mathbf{R}; \mathbf{r}) \rangle_N$, so that the $F - F_{\text{id}}$ is a reduced variance estimator [18] of the difference: $f_N - f_{\text{id}}$.

There is a problem with projecting methods to calculate properties other than the energy. Forward walking or reweighting methods based on using Ψ_β in Eq. (2) become very inefficient for long projection time, since the variance increases exponentially with β . To avoid this problem, mixed estimators, based on $\Psi_\beta \Psi_0$, are frequently used but they can introduce a systematic bias. Unbiased estimators for the pair correlation function, potential, and kinetic energy have been obtained within RMC calculations [12]. Based on a generalized partition function, Q , we extend RMC calculations to include sampling of off-diagonal matrix elements [10]

$$Q = \int d\mathbf{R} |\Psi_{\beta/2}(\mathbf{R})|^2 + \frac{s}{N} \sum_i \int \frac{d\mathbf{r}}{V} \int_0^\beta \frac{d\tau}{\beta} \int d\mathbf{R} |\Psi_{\beta-\tau}(\mathbf{R}) \Psi_\tau(\mathbf{R}; \mathbf{r}_i + \mathbf{r})|, \quad (5)$$

where s is a parameter used to optimize the efficiency ($s = 0$ corresponds to the usual diagonal RMC calculations [12]). Similar to the worm algorithm used in continuous path-integral calculations [11], our calculations include moves which ‘‘open’’ (or ‘‘close’’) a path from diagonal space \mathbf{R} to off-diagonal space $(\mathbf{R}, \mathbf{r}_i + \mathbf{r})$. Such moves are included at $\tau = 0$ and ‘‘propagated’’ by reptation moves [12,19] to the interior of the path ($\tau > 0$). In contrast to previous calculations using so-called mixed estimators [6], this generalization gives an unbiased estimator of the off-diagonal density matrix, $f_N(\mathbf{r})$, and the momentum distribution, $n_{\mathbf{k}}^N$. Reduction of the variance based on the considerations above, Eq. (4), is still possible, but less effective.

Quantum Monte Carlo results are obtained for typically $N \lesssim 10^3$ electrons. The extrapolation to the thermodynamic limit introduces important quantitative and qualitative changes of the momentum distribution around the Fermi surface, k_F [9]. For a homogeneous periodic system, the orbitals are plane waves, $\phi_n(\mathbf{r}) = \exp[i(\mathbf{k}_n + \vec{\theta}) \cdot \mathbf{r}]$, in the Slater determinant of Eq. (1), where $\mathbf{k}_j \in \mathbf{G}_N \equiv \{(n_1, n_2, n_3)2\pi V^{-1/3}\}$ with integer n_i , and $\vec{\theta}$ can be chosen to introduce twisted boundary conditions [8,20]. For a normal Fermi liquid, we further have $|\mathbf{k}_j + \vec{\theta}| \leq k_F$, and the generalized backflow and Jastrow potential W_N and U_N can be written exclusively in terms of collective coordinates $\rho_{\mathbf{k}} = \sum_n e^{i\mathbf{k} \cdot \mathbf{r}_n}$ and their gradients [7,16]. Using the wave function ‘‘potentials,’’ W_N and U_N , expressed as continuous functions in terms of the collective coordinates, the relation between the wave function in the limit $N \rightarrow \infty$ to a finite system is well defined, as it just amounts to evaluations on a denser grid in \mathbf{k} space [8,9].

Let us first discuss the finite size scaling for a Slater-Jastrow (SJ) wave function: a determinant with $W_N \equiv 0$, together with a two-body Jastrow correlation, $U_N = \sum_k u_k \rho_k \rho_{-k} / 2V$. We further assume that the function u_k is analytically given. In our SJ-VMC calculations, we use the Gaskell form $2nu_k^{\text{SJ}} \equiv -S_0^{-1}(k) + [S_0^{-2}(k) + 2nv_k/\varepsilon_k]^{1/2}$ where $S_0(k)$ is the ideal gas structure factor, $v_k = 4\pi e^2/k^2$, and $\varepsilon_k = \hbar^2 k^2 / 2m$ [21,22]. Neglecting mode coupling between single-particle modes in D_N and collective modes described by U_N , the single-particle density matrix, Eq. (2), can be approximated as

$$f_N(\mathbf{r}) \approx f_c(\mathbf{r}) \equiv \left\langle \frac{D'_N}{D_N} \right\rangle_N \langle e^{-(U'_N - U_N)} \rangle_N, \quad (6)$$

where the prime indicates the off-diagonal configuration, e.g., $D'_N \equiv D_N(\mathbf{R}; \mathbf{r}_1 + \mathbf{r})$. Within the cumulant and rotating wave approximation, we then obtain an explicit expression,

$$f_c(\mathbf{r}) \approx f_{\text{id}}(r) \exp[-x_N(r)], \quad (7)$$

TABLE I. The total (E), potential (V), and kinetic energy (T) per particle in Ry, and the contact value of the pair correlation function $g(0)$, all extrapolated to the thermodynamic limit from unbiased RMC calculations with BF nodes. We further give parameters of the momentum distribution at small k (n_0 , and n_2), $n(k \rightarrow 0) = n_0 - n_2(k/k_F)^2$, and at k_F , $\bar{n} = [n(k_F^+) + n(k_F^-)]/2$.

r_s	1	2	3.99	5	10
E	1.173(2)	0.0039(1)	-0.1555(1)	-0.1520(1)	-0.1071(1)
T	2.290(3)	0.6024(5)	0.1688(1)	0.1131(1)	0.0349(1)
V	-1.116(1)	-0.5985(1)	-0.3243(1)	-0.2651(1)	-0.1421(1)
$g(0)$	0.268(3)	0.152(2)	0.057(2)	0.034(1)	0.0036(4)
n_0	0.999	0.998	0.97	0.93	0.88
n_2	0.038	0.066	0.12	0.098	0.21
\bar{n}	0.490	0.477	0.460	0.456	0.414

$$x_N(r) = \frac{1}{V} \sum_{|\mathbf{k}| \leq k_c} [u_k(S_k - 1) + nu_k^2 S_k][e^{i\mathbf{k}\cdot\mathbf{r}} - 1], \quad (8)$$

where $S_k = \langle \rho_{\mathbf{k}} \rho_{-\mathbf{k}} \rangle_N / N$ is the structure factor, $f_{\text{id}}(r) = 2 \sum_{\mathbf{k} \leq k_c} e^{i\mathbf{k}\cdot\mathbf{r}} / N$ is the single-particle density matrix of the corresponding ideal gas, and we have neglected contributions of short wavelength modes, $k_c \approx 0.48 r_s^{1/2} k_F$ [23]. Further, we can use $S_k \approx [2nu_k + 1/S_0(k)]^{-1}$ to express S_k in terms of u_k and $S_0(k)$, which is based on assuming Gaussian statistics for $\rho_{\mathbf{k}}$, so that Eq. (7) gives an explicit expression for $f_N(\mathbf{r}) \approx f_c(\mathbf{r})$ in terms of a given Jastrow factor. Whereas the resulting model, Eq. (7), depends weakly on k_c , so that $f_N(r)$ and n_k are only qualitatively described, the size extrapolation is quantitatively correct, as it is dominated by the Jastrow singularity $u_k \rightarrow (v_k/2n\varepsilon_k)^{1/2}$ and $S_k \rightarrow (2nv_k/\varepsilon_k)^{-1/2}$ for $k \rightarrow 0$ stemming from the plasmon contributions.

Since we expect that mode coupling is negligible in the long wavelength limit, the cumulant expression, Eq. (7), can be used to determine the size corrections of QMC calculations of the finite system

$$f_{\infty}(\mathbf{r}) = \frac{2}{n} \int \frac{d^3k}{(2\pi)^3} n_k^N e^{i\mathbf{k}\cdot\mathbf{r}} e^{-(x_{\infty}(r) - x_N(r))}. \quad (9)$$

Here n_k^N is the momentum distribution of the N electron system, defined for all values of \mathbf{k} in a grand canonical ensemble using twisted boundary conditions [8]. Using the long-range properties of u_k and S_k , $x_{\infty}(r)$ is obtained from Eq. (8) in the limit $N \rightarrow \infty$. From the Fourier transform of $f_{\infty}(\mathbf{r})$, Eq. (9), we obtain the extrapolated momentum distribution, n_k^{∞} . A related linearized expression has been used to extrapolate n_k of the two-dimensional electron gas using BF-VMC [9] calculations.

Following the analysis of Ref. [9], leading order corrections to the renormalization factor, $Z_N = n_{k_F^-}^N - n_{k_F^+}^N$, are given by

$$Z_{\infty} \approx Z_N \exp[-\Delta_N]$$

$$\begin{aligned} \Delta_N &= \int_{-\pi/L}^{\pi/L} \frac{d^3q}{(2\pi)^3} \frac{u_q}{2} [1 + \mathcal{O}([2nu_q S_0(q)]^{-1})] \\ &= c \left(\frac{3}{4\pi}\right)^{1/3} \left(\frac{r_s}{3}\right)^{1/2} N^{-1/3} + \mathcal{O}(N^{-2/3}), \end{aligned} \quad (10)$$

where $c \approx 1.221$ is a numerical factor to account for the cubic integration volume [24]. Whereas the asymptotic region is only reached for large systems with $N^{1/3} r_s^{1/2} \gg 1$, the extrapolation based on the full expression, Eq. (9), includes corrections beyond the leading order term. Analyzing Eq. (9) around k_F , we obtain the exact leading order behavior with an infinite slope at k_F :

$$\begin{aligned} n(k \rightarrow k_F^{\pm}) &\approx n(k_F^{\pm}) \\ &+ \frac{Z_{\infty}}{2\pi} \left(\frac{9\pi}{4}\right)^{1/3} \sqrt{\frac{r_s}{3}} \left[\frac{k}{k_F} - 1\right] \log \left| \frac{k}{k_F} - 1 \right|. \end{aligned} \quad (11)$$

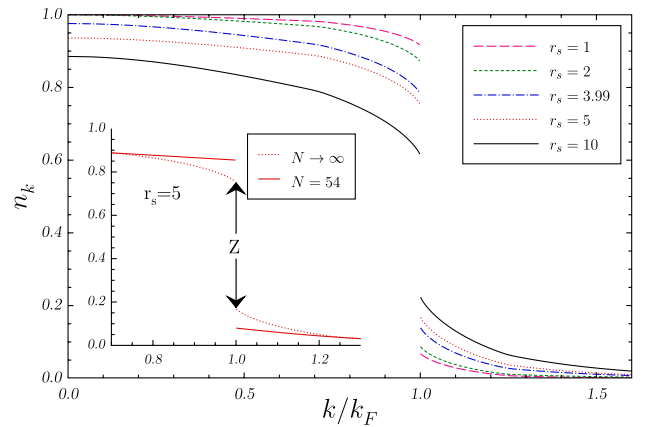


FIG. 1 (color online). The momentum distribution (n_k) of the unpolarized electron gas for various densities extrapolated to the thermodynamic limit. The inset shows the extrapolation of n_k for $r_s = 5$ from a system with $N = 54$ electrons to the thermodynamic limit, $N \rightarrow \infty$, leading to a significant reduction of the renormalization factor Z .

TABLE II. Renormalization factor, Z , extrapolated to the thermodynamic limit from unbiased RMC calculations with backflow nodes (BF-RMC), together with SJ-VMC and BF-VMC results, compared with perturbative results from literature. Previous SJ-DMC results [6] used mixed estimators without thermodynamic limit extrapolation.

r_s	1	2	3.99	5	10
BF-RMC	0.84(2)	0.77(1)	0.64(1)	0.58(1)	0.40(1)
SJ-VMC	0.894(9)	0.82(1)	0.69(1)	0.61(2)	0.45(1)
BF-VMC	0.86(1)	0.78(1)	0.65(1)	0.59(1)	0.41(1)
G_0W_0 [25]	0.859	0.768	0.646 ^a	0.602	0.45
GW_0 [26]		0.804	0.702 ^a		
GW [27]		0.846	0.793 ^a		
Lam [28]	0.896	0.814	0.615 ^a	0.472	
Random phase approximation (RPA)[28]	0.843	0.700	0.442 ^a	0.323	
SJ-DMC [6]	0.952	0.889		0.725	0.593

^aLiterature values are at $r_s = 4$ instead of $r_s = 3.99$.

Size extrapolation, discussed above, requires the knowledge of the structure factor, S_k , and the Jastrow potential, u_k , in Eq. (8). The QMC calculation of the N -particle system allows us only to determine them on a finite grid in \mathbf{k} space, but the analytic continuation to the dense grid can be done by interpolation from their known behavior at small k [8]. Whereas S_k can be calculated directly, $u_k = u_k^{\text{SJ}}$ is only known explicitly for VMC calculations using a Slater-Jastrow trial function. In general, imaginary time projection and backflow introduce an effective Jastrow potential, u_k , different from the explicitly given form of the underlying trial wave function. Expecting small changes at long wavelength, $u_k = u_k^{\text{SJ}} + \delta u_k$, we obtain the modifications δu_k from changes in the structure factor $\delta S_k = S_k - S_k^{\text{SJ}}$ by linear response. For our purpose, mode coupling can be neglected, as well as deviations from Gaussian statistics, so that $\delta S_k / \delta u_{k'} \simeq -2n S_k^{-2} \delta_{\mathbf{k}, \mathbf{k}'}$ for $k \rightarrow 0$. Modifications due to δu_k have been used to estimate the systematic error of the finite size extrapolation.

Using SJ-VMC calculations with u_k^{SJ} for $N = 54$ to $N = 1024$ electrons, we have checked that size extrapolations based on Eq. (9) with $N = 54$ are reliable. We have further checked for larger systems ($N = 342$) that our backflow wave functions and the imaginary time projection do not modify the long-range behavior already present in SJ-VMC calculations, so that the analysis above can be also applied to BF-VMC and RMC calculations. Thus, the more expensive backflow VMC and RMC calculations based on the analytical wave functions in Ref. [7] are only done with $N = 54$. Extrapolated results on the total energy E , unbiased estimators from reptation for the potential (V) and kinetic energies (T), and the contact value of the pair correlation function, $g(0)$, are given in Table I. The momentum distribution is shown in Fig. 1. The values for the renormalization factor, Z , together with different perturbative results from the literature are given in Table II. Note that the BF-VMC value $Z = 0.66(2)$ at $r_s = 3.99$ of Ref. [5] was based on the extrapolation of systems

containing up to $N = 342$ electrons. This is an explicit check on the extrapolation procedure. Table I also contains the values of the momentum distribution at the origin, n_0 , the negative slope at the origin, n_2 , and $\bar{n} = (n_{k_F^-} + n_{k_F^+})/2$. These values can be used to parametrize the momentum distribution along the lines given in Ref. [29], together with Z , the exact large k asymptotics [30], $n(k \rightarrow \infty) = (9/2)r_s^2 g(0)/k^8$, and the exact behavior close to the Fermi surface, Eq. (11). Whereas the mixed estimator usually employed in DMC calculations introduces a small bias in the momentum distribution, size extrapolation introduces large systematic modifications which limit the precision of the calculations. Previous DMC results [6], using mixed estimators and SJ nodes, suffer from these strong finite size effects and overestimate Z by a large amount.

In summary, we have calculated the momentum distribution using a new unbiased and much more accurate Monte Carlo method, and extrapolated the results to the thermodynamic limit. In particular, our data allow a quantitative comparison of the renormalization factor, Z , with approximate calculations (see Table II). The excellent agreement of our results with G_0W_0 [25,31,32] over the whole metallic density region $r_s \lesssim 5$ strongly indicates that vertex corrections and self-consistency issues – neither is included in G_0W_0 —are canceling each other, at least close to the Fermi surface.

Computer time at CNRS-IDRIS is acknowledged, Project No. IDRIS 061801. C. P. is supported by IIT under the SEED project grant number 259 SIMBEDD.

-
- [1] D. M. Ceperley and B. J. Alder, *Phys. Rev. Lett.* **45**, 566 (1980).
 - [2] P. Hohenberg and W. Kohn, *Phys. Rev.* **136**, B864 (1964); W. Kohn and L. J. Sham, *Phys. Rev.* **140**, A1133 (1965).
 - [3] P. Nozières, *Theory of Interacting Fermi Systems* (W. A. Benjamin, Inc., New York, 1964).

- [4] T. L. Gilbert, *Phys. Rev. B* **12**, 2111 (1975); P. O. Lodwin, *Phys. Rev.* **97**, 1474 (1955).
- [5] S. Huotari *et al.*, *Phys. Rev. Lett.* **105**, 086403 (2010).
- [6] G. Ortiz and P. Ballone, *Phys. Rev. B* **50**, 1391 (1994); **56**, 9970 (1997).
- [7] M. Holzmann *et al.*, *Phys. Rev. E* **68**, 046707 (2003).
- [8] S. Chiesa *et al.*, *Phys. Rev. Lett.* **97**, 076404 (2006).
- [9] M. Holzmann *et al.*, *Phys. Rev. B* **79**, 041308 (2009).
- [10] G. Carleo *et al.*, *Phys. Rev. E* **82**, 046710 (2010).
- [11] M. Boninsegni, Nikolay Prokof'ev, and B. Svistunov, *Phys. Rev. Lett.* **96**, 070601 (2006).
- [12] S. Baroni and S. Moroni, *Phys. Rev. Lett.* **82**, 4745 (1999).
- [13] B. Militzer and E. L. Pollock, *Phys. Rev. Lett.* **89**, 280401 (2002); B. Militzer *et al.*, arXiv:cond-mat/0310401.
- [14] S. Moroni and M. Boninsegni, *J. Low Temp. Phys.* **136**, 129 (2004).
- [15] J. Kolorenc and L. Mitas, *Rep. Prog. Phys.* **74**, 026502 (2011).
- [16] M. Holzmann, B. Bernu, and D. M. Ceperley, *Phys. Rev. B* **74**, 104510 (2006).
- [17] W. L. McMillan, *Phys. Rev.* **138**, A442 (1965).
- [18] This variance reduction can be generalized to periodic systems with Bloch orbitals, $\phi_{n\mathbf{k}}(\mathbf{r}) \propto e^{i\mathbf{k}\cdot\mathbf{r}}\varphi_n(\mathbf{r})$, displacing only the phase in the determinant, $\phi_{n\mathbf{k}}(\mathbf{r}_i) \rightarrow e^{i\mathbf{k}\cdot\mathbf{r}}\phi_{n\mathbf{k}}(\mathbf{r}_i)$, when $\mathbf{r}_i \rightarrow \mathbf{r}_i + \mathbf{r}$.
- [19] C. Pierleoni and D. M. Ceperley, *Chem. Phys. Chem.* **6**, 1872 (2005).
- [20] C. Lin, F. H. Zong, and D. M. Ceperley, *Phys. Rev. E* **64**, 016702 (2001).
- [21] T. Gaskell, *Proc. Phys. Soc. London* **77**, 1182 (1961); **80**, 1091 (1962).
- [22] D. M. Ceperley, *Phys. Rev. B* **18**, 3126 (1978).
- [23] D. Bohm and D. Pines, *Phys. Rev.* **92**, 609 (1953); D. Pines, *Elementary Excitations in Solids* (Perseus Books, Reading, MA, 1969).
- [24] M. Holzmann *et al.*, arXiv:1105.2964.
- [25] L. Hedin, *Phys. Rev. A* **139**, A796 (1965).
- [26] U. von Barth and B. Holm, *Phys. Rev. B* **55**, 10120(E) (1997); **55**, 12902 (1997).
- [27] B. Holm and U. von Barth, *Phys. Rev. B* **57**, 2108 (1998).
- [28] J. Lam, *Phys. Rev. B* **3**, 3243 (1971).
- [29] P. Ziesche, *Phys. Status Solidi B* **232**, 231 (2002); P. Gori-Giorgi and P. Ziesche, *Phys. Rev. B* **66**, 235116 (2002).
- [30] J. C. Kimball, *J. Phys. A* **8**, 1513 (1975); H. Yasuhara and Y. Kawazoe, *Physica (Amsterdam)* **85A**, 416 (1976).
- [31] G. E. Simion and G. F. Giuliani, *Phys. Rev. B* **77**, 035131 (2008).
- [32] T. M. Rice, *Ann. Phys. (N.Y.)* **31**, 100 (1965).